Electromagnetic time constants of the Earth's mantle

Jens Stadelmann & Peter Weidelt

Institut für Geophysik und Extraterrestrische Physik
Technische Universität Braunschweig

1. Introduction and Summary

By electromagnetic induction in the mantle, the geomagnetic secular variation (SV) is distorted on its passage from the Core-Mantle Boundary (CMB) to the surface of the Earth: It gets delayed, broadened and skewed. An investigation of the impact of mantle conductivity on the backpropagation of the observed SV to the CMB is of interest for instance for an inference of the tangential fluid flow in the core close to the CMB from a reliable knowledge of the radial magnetic field component and its time variation at the CMB [e.g., Benton & Whaler (1983), Ballani et al. (2002)]. There have been also some indications that the diffusion of the SV through the mantle can give some relevant constraints on the poorly known Lower Mantle conductivity [e.g., McDonald (1957), Backus (1983), Holme (1998)].

For the diffusion of the SV, all reasonable models of mantle conductivity qualify the mantle as a *weak* conductor, since all relevant time constants of mantle diffusion (see Sect. 3) as free-decay time of current systems, delay, smoothing and skewing time of an impulse propagating from the CMB upwards, are at most of the order 100 -200 days (see Tables 2 and 3) and therefore are small compared with the time scale of SV (decades of years).

We express in Sect. 3.3 delay, smoothing and skewing times in terms of integrals over the mantle conductivity and show in Sect. 3.4 that simple relations exist between these times and the times of free decay of mantle currents. – Although formally two sets of time constants for radial and tangential magnetic components exist, the boundary conditions at the CMB attribute a geophysical significance as delay time only to the former.

2. Basic equations

We assume spherical coordinates (r, ϑ, φ) with the CMB at $r = c$ and the surface of the Earth at $r = a$. Let $\sigma = \sigma(r)$ be the conductivity distribution with $\sigma(r) = \infty$ for $r < c$ and

$\sigma(r) = 0$ for $r > a$. Neglecting displacement currents and using at first a harmonic time dependence $\sim \exp(i\omega t)$, the basic differential and constituitive laws are

$$\nabla \times \mathbf{H} = \mathbf{J}, \qquad \nabla \times \mathbf{E} = -i\omega\mathbf{B} \tag{2.1}$$

and

$$\mathbf{B} = \mu_0\mathbf{H}, \qquad \mathbf{J} = \sigma\mathbf{E}, \tag{2.2}$$

where **H**, **B**, **E** and **J** are, respectively, the vectors of the magnetic field, the magnetic flux density, the electric field and the electric current density.

Since $\nabla \cdot \mathbf{B} = 0$ and $\nabla \cdot \mathbf{J} = 0$, the solenoidal vectors **B** and **J** admit a Mie decomposition into a poloidal and toroidal part. For **B** this decomposition is

$$\mathbf{B} = \boldsymbol{\nabla}\times\boldsymbol{\nabla}\times(\mathbf{r}P_B) + \boldsymbol{\nabla}\times(\mathbf{r}T_B). \tag{2.3}$$

Because of

$$B_r = -r\nabla_s^2 P_B, \quad \mu_0 J_r = -r\nabla_s^2 T_B, \tag{2.4}$$

these components depend on one scalar only. Here ∇_s^2 is the tangential part of the Laplace operator, which does not involve differentation in r-direction. The knowledge of B_r and J_r therefore allows a separate determination of P_B and T_B. Generally, lateral non-uniformities inside the mantle couple the scalars P_B and T_B. However, under the present assumption that the conductivity depends on r only, these modes are not getting mixed inside the layered mantle and therefore satisfy uncoupled differential equations

$$\nabla^2 P_B = i\omega\mu_0\sigma(r)P_B, \qquad \nabla^2 T_B - \frac{\sigma'(r)}{r\sigma(r)}\partial_r(rT_B) = i\omega\mu_0\sigma(r)T_B. \tag{2.5}$$

The continuity of the tangential components of **B** and **E** at layer boundaries requires the continuity of

$$\partial_r P_B, \quad P_B, \quad T_B \quad \text{and} \quad \sigma^{-1}\partial_r(rT_B). \tag{2.6}$$

Since $J_r(r) = 0$ in $r \geq a$, the condition $J_r(a) = 0$ implies according to (2.4) that $T_B(a) = 0$. Therefore the toroidal part of **B** vanishes at $r = a$ and the observed surface magnetic field is purely poloidal.

Now we have to discuss the boundary conditions for P_B at $r = c$ and for $r \to \infty$. On the surface $r = c$ of the perfectly conducting core the radial component B_r of the currents induced in the mantle will vanish. Therefore at the CMB B_r is presented by the pure SV source field B_r^{SV}, created by the fluid motion in the core. With (2.4) this gives rise to the boundary condition

$$-c\nabla_s^2 P_B(r = c) = B_r^{SV}, \tag{2.7}$$

where the source B_r^{SV} is assumed to be given. Since **B** has to vanish for $r \to \infty$, we have at infinity the boundary condition

$$P_B(r) \to 0 \quad \text{for} \quad r \to \infty. \tag{2.8}$$

In the case of a layered mantle it is not necessary to exclude current leakage from the core into the mantle, because this poloidal current flow gives rise to a toroidal magnetic field only, which cannot be seen at the surface of the Earth. This is different for a mantle with lateral non-uniformities, where the non-uniformity can partially convert the toroidal magnetic source field into a poloidal mode, which then is observable at the surface of the Earth.

The well-known general solution of the left equation of (2.5) in spherical coordinates is

$$P_B(r,\vartheta,\varphi) = \frac{1}{r}\sum_{\ell=1}^{\infty} f_\ell(r)\, S_\ell(\vartheta,\varphi), \tag{2.9}$$

where $S_\ell(\vartheta,\varphi)$ is a spherical harmonic of degree ℓ and $f_\ell(r)$ is a solution of the ordinary differential equation

$$f_\ell''(r) = \left[\frac{\ell(\ell+1)}{r^2} + i\omega\mu_0\sigma\right] f_\ell(r). \tag{2.10}$$

An additional term $\ell = 0$ in (2.9) would depend on r only and therefore does not contribute when forming **B** according to (2.3).

In the following we are considering ratios of corresponding spectral field components at $r = a$ and $r = c$. Let

$$P_{B\ell}(r,\vartheta,\varphi) := \frac{1}{r} f_\ell(r) S_\ell(\vartheta,\varphi).$$

a spectral component of P_B of degree ℓ. Then (2.3) yields

$$B_{\ell r}(r,\vartheta,\varphi) = \frac{\ell(\ell+1)}{r^2}\, f_\ell(r)\, S_\ell(\vartheta,\varphi), \tag{2.11}$$

$$B_{\ell\vartheta}(r,\vartheta,\varphi) = \frac{1}{r}\, f_\ell'(r)\, \partial_\vartheta S_\ell(\vartheta,\varphi), \tag{2.12}$$

$$B_{\ell\varphi}(r,\vartheta,\varphi) = \frac{1}{r\sin\vartheta}\, f_\ell'(r)\, \partial_\varphi S_\ell(\vartheta,\varphi), \tag{2.13}$$

where $f(r)$ is a solution of (2.10) vanishing for $r \to \infty$. Then the transfer functions $\Gamma_\ell^R(\omega)$ and $\Gamma_\ell^T(\omega)$ for the radial and tangential magnetic components are defined as

$$\Gamma_\ell^R(\omega) := \frac{B_{\ell r}(a,\vartheta,\varphi)}{B_{\ell r}(c,\vartheta,\varphi)} = \frac{c^2}{a^2}\cdot\frac{f_\ell(a,\omega)}{f_\ell(c,\omega)}, \tag{2.14}$$

$$\Gamma_\ell^T(\omega) := \frac{B_{\ell\vartheta}(a,\vartheta,\varphi)}{B_{\ell\vartheta}(c,\vartheta,\varphi)} = \frac{B_{\ell\varphi}(a,\vartheta,\varphi)}{B_{\ell\varphi}(c,\vartheta,\varphi)} = \frac{c}{a}\cdot\frac{f_\ell'(a,\omega)}{f_\ell'(c,\omega)}. \tag{2.15}$$

In the 'low-induction' case, defined by $\omega\mu_0\sigma(r)r^2 \ll \ell(\ell+1)$ in $c < r < a$, the appropriate solution of (2.10) is $f_\ell(r) \sim r^{-\ell}$ and therefore in this limit

$$\Gamma_\ell^R = \Gamma_\ell^T = (c/a)^{\ell+2}. \tag{2.16}$$

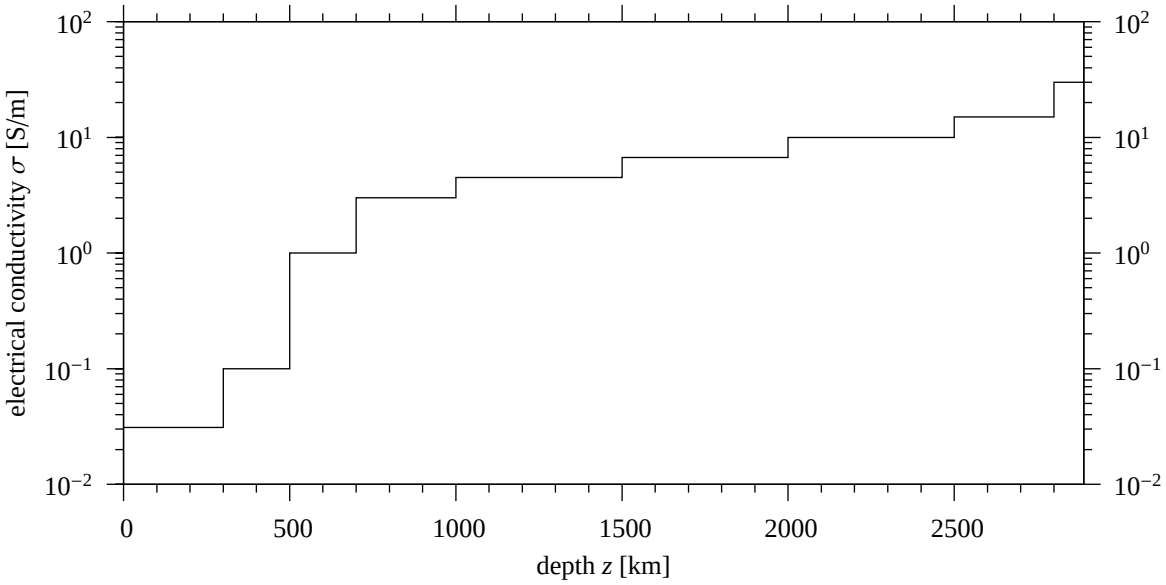

Figure 1: Model of the electrical conductivity in the layered mantle.

Now we shall express the radial and tangential components at $r = c$ and $r = a$ in terms of the SV source field and $\Gamma^{R,T}(\omega)$. The source enters via (2.7). The expansion of the given B_r^{SV} into spherical harmonics is

$$B_r(c,\vartheta,\varphi,\omega) = B_r^{SV}(\vartheta,\varphi,\omega) = \sum_{\ell=1}^{\infty} S_\ell^{SV}(\vartheta,\varphi,\omega). \tag{2.17}$$

For a single degree ℓ we obtain

$$\begin{aligned} B_{\ell r}(c,\vartheta,\varphi,\omega) &= S_\ell^{SV}(\vartheta,\varphi,\omega), & B_{\ell\vartheta}(c,\vartheta,\varphi,\omega) &= -\frac{1}{\ell+1}\cdot\frac{\Gamma_\ell^R(\omega)}{\Gamma_\ell^T(\omega)}\cdot\partial_\vartheta S_\ell^{SV}(\vartheta,\varphi,\omega), \\ B_{\ell r}(a,\vartheta,\varphi,\omega) &= \Gamma_\ell^R(\omega)\, S_\ell^{SV}(\vartheta,\varphi,\omega), & B_{\ell\vartheta}(a,\vartheta,\varphi,\omega) &= -\frac{1}{\ell+1}\cdot\Gamma_\ell^R(\omega)\cdot\partial_\vartheta S_\ell^{SV}(\vartheta,\varphi,\omega). \end{aligned} \tag{2.18}$$

A typical conductivity model, for which we like to compute the transfer functions $\Gamma_\ell^R(\omega)$ and $\Gamma_\ell^T(\omega)$ is the 9-layer model shown in Fig. 1.

3. Time constants of mantle diffusion

3.1. General ideas

In this section it is investigated, how a geomagnetic signal, diffusing from the CMB upwards, is distorted by the conductivity of the mantle. The action of the mantle as a low-pass filter for the SV has been investigated in great depth and detail by Backus (1983).

The present more elementary approach resumes Backus' concept of delay and smoothing times, adds the skewness time quantifying asymmetry and links all time constants to the free-decay times. Moreover, attention is drawn to the existence of two sets of time constants both for the radial and tangential magnetic component. Due to the boundary condition (2.7) at the perfectly conducting core, however, only the radial time-constants describe the delayed arrival of an impulse originating from the CMB.

Let $B_\ell(r,t)$ and $B_\ell(r,\omega)$ be generic magnetic field components in the time and frequency domain and let $\Gamma_\ell(\omega)$ the generic version of the transfer functions (2.14) and (2.15). Then we have in the frequency domain

$$B_\ell(a,\omega) = \Gamma_\ell(\omega) B_\ell(c,\omega) \tag{3.19}$$

and therefore in the time domain

$$B_\ell(a,t) = \int_{-\infty}^{t^+} B_\ell(c,t')\gamma_\ell(t-t')\,dt' \tag{3.20}$$

where the convolution kernel $\gamma_\ell(t)$ is the Fourier transform of $\Gamma_\ell(\omega)$,

$$\gamma_\ell(t) = \frac{1}{2\pi}\int_{-\infty}^{+\infty} \Gamma_\ell(\omega)\mathrm{e}^{i\omega t}\,d\omega. \tag{3.21}$$

In (3.20) we have already made use of fact that $\gamma_\ell(t)$ is a causal function satisfying $\gamma_\ell(t) = 0$ for $t < 0$. Formally this follows from the fact that $\Gamma_\ell(\omega)$ is analytic outside the positive imaginary axis. On this semiaxis are lying at $\omega = i\lambda_{\ell j}$, $\lambda_{\ell j} > 0$, an infinite number of poles, briefly examined in Sect. 3.4. [The poles of $\Gamma_\ell^R(\omega)$ define the decay constants of freely decaying mantle-current systems of degree ℓ.] For $t < 0$ the contour in (3.21) can be closed by a large semicircle in the lower ω-halfplane, which does not contribute to the integral. From the analyticity of $\Gamma_\ell(\omega)$ in the semicircle then follows the causality of $\gamma_\ell(t)$.

For the conductivity model of Fig. 1 the convolution kernels $\gamma_\ell^R(t)$ and $\gamma_\ell^T(t)$ are shown in Fig. 2 for the first three degrees.
From the inversion of (3.21),

$$\Gamma_\ell(\omega) = \int_0^\infty \gamma_\ell(t)\mathrm{e}^{-i\omega t}\,dt, \tag{3.22}$$

follows with (2.16), i.e. with $\Gamma_\ell^R(0) = \Gamma_\ell^T(0) = (c/a)^{\ell+2}$, that

$$\int_0^\infty \gamma_\ell^R(t)\,dt = \int_0^\infty \gamma_\ell^T(t)\,dt = (c/a)^{\ell+2}. \tag{3.23}$$

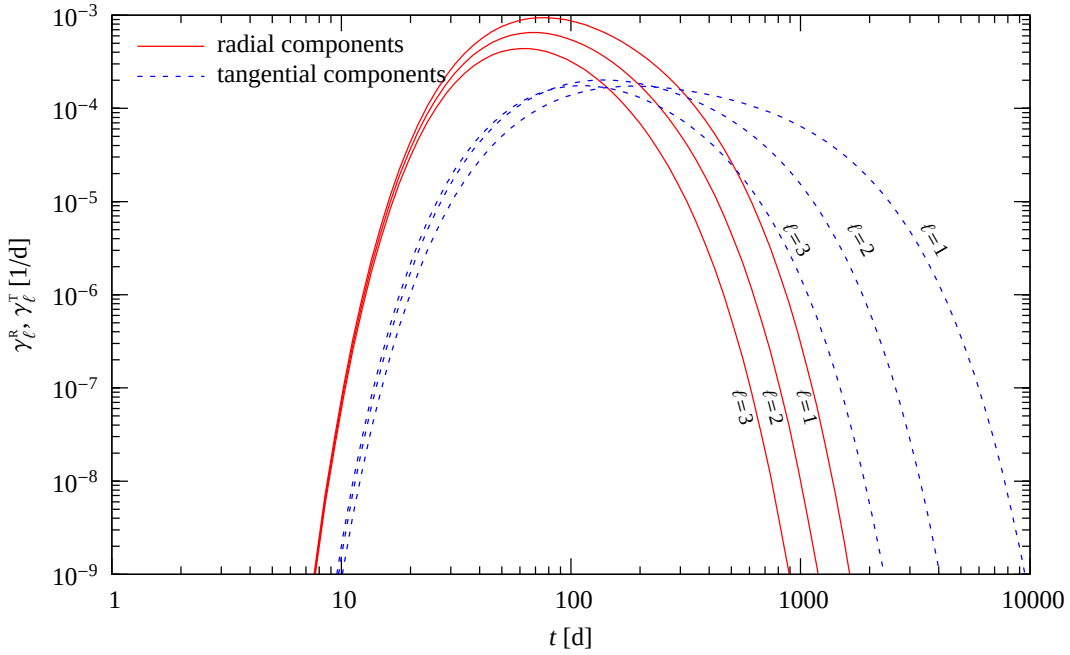

Figure 2: Convolution kernels $\gamma_\ell^R(t)$ and $\gamma_\ell^T(t)$ for the first three degrees derived from the conductivity model of Fig. 1. The logarithmic scales mask the relation (3.23).

Physically, $\gamma_\ell^R(t)$ is the delayed, broadened and skewed surface response to a $\delta(t)$-impulse in the magnetic radial component at the CMB. The stronger delayed and smoothed response $\gamma_\ell^T(t)$ has no obvious physical meaning. However, its important role in the propagation of the tangential components from $r = c$ to the surface $r = a$ via the convolution integral (3.20) is elucidated in Sect. 3.2.

Delay, broadening and skewness of the 'probability density distribution' $\gamma(t)/\Gamma_\ell(0)$ can be expressed, respectively, by the time constants τ_ℓ, σ_ℓ and ϱ_ℓ, which are derived from the first three moments of $\gamma(t)/\Gamma_\ell(0)$. Let $m_{\ell k}$ and $\mu_{\ell k}$ be the k-th moments about $t = 0$ and about the mean, i.e.

$$\Gamma_\ell(0)\, m_{\ell k} := \int_0^\infty \gamma_\ell(t)\, t^k\, dt = \left.\frac{d^k \Gamma_\ell(\omega)}{d(-i\omega)^k}\right|_{\omega=0}, \quad \Gamma_\ell(0)\, \mu_{\ell k} := \int_0^\infty \gamma_\ell(t)\, (t-\tau_\ell)^k\, dt \qquad (3.24)$$

with $\tau_\ell := m_{\ell 1}$. The connection between $m_{\ell k}$ and $\mu_{\ell k}$ is

$$m_{\ell 1} = \tau_\ell, \quad m_{\ell 2} = \mu_{\ell 2} + \tau_\ell^2, \quad m_{\ell 3} = \mu_{\ell 3} + 3\mu_{\ell 2}\tau_\ell + \tau_\ell^3. \qquad (3.25)$$

With the further definitions

$$\sigma_\ell^2 := \mu_{\ell 2}, \quad \varrho_\ell^3 := \mu_{\ell 3} \qquad (3.26)$$

the time constants are reversely given by

$$\tau_\ell = m_{\ell 1}, \quad \sigma_\ell^2 = m_{\ell 2} - m_{\ell 1}^2, \quad \varrho_\ell^3 = m_{\ell 3} - 3m_{\ell 2}m_{\ell 1} + 2m_{\ell 1}^3, \tag{3.27}$$

The skewness ϱ_ℓ^3 can have both signs, where a positive skewness denotes a long tail of $\gamma_\ell(t)$ in direction of increasing t. An inspection of Fig. 2 shows that this case has to be expected. According to (3.24) a low-frequency approximation of $\Gamma_\ell(\omega)$ with an approximation error of $O(\omega^4)$ is

$$\begin{aligned} \Gamma_\ell(\omega) &\simeq \Gamma_\ell(0)\,[\,1 + (-i\omega)\,m_{\ell 1} + (-i\omega)^2\,m_{\ell 2}/2 + (-i\omega)^3\,m_{\ell 3}/6\,] \qquad (3.28)\\ &= \Gamma_\ell(0)\,[\,1 + (-i\omega)\tau_\ell + (-i\omega)^2\,(\mu_{\ell 2} + \tau_\ell^2)/2 + (-i\omega)^3\,(\mu_{\ell 3} + 3\mu_{\ell 2}\tau_\ell + \tau_\ell^3)/6\,]. \end{aligned}$$

This low-frequency approximation applies, if the characteristic time constant T_{SV} of the secular variation (i.e. $\omega = 1/T_{SV}$) is much larger than the time constants τ_ℓ, σ_ℓ and ϱ_ℓ, which are properties of the mantle and therefore depend on conductivity only. Table 2 gives for the model of Fig. 1 mantle time constants less than 1000 days, whereas T_{SV} will be at least decades of years. In this case the B_r-signal at $r = a$ will be essentially a replica of the signal at the CMB, reduced by the geometric factor $\Gamma_\ell(0)$ and delayed by τ_ℓ. The two higher order terms in (3.28) introduce some broadening and skewing.

The first three moments fix only the given terms in the power series (3.28) and leave $\gamma_\ell(t)$ non-unique. We shall briefly consider only two different choices:

- **Skewed Gaussian distribution**

$$\begin{aligned} \Gamma_\ell(\omega) &\simeq \Gamma_\ell(0)\exp[\,(-i\omega)\tau_\ell + (-i\omega)^2\,\mu_{\ell 2}/2 + (-i\omega)^3\,\mu_{\ell 3}/6\,] \qquad (3.29)\\ &= \Gamma_\ell(0)\exp[\,(-i\omega)\tau_\ell + (-i\omega)^2\,\sigma_\ell^2/2 + (-i\omega)^3\,\varrho_\ell^3/6\,], \qquad (3.30) \end{aligned}$$

  If also fourth moments are included, the first neglected term in the exponent of (3.29) would be of the more complicated form $(-i\omega)^4(\mu_4 - 3\mu_2^2)/24$ (Backus 1983, p. 719; Fisz 1976, p. 139), where the expression $\mu_4 - 3\mu_2^2$ is the *excess* or *kurtosis*, vanishing for a Gaussian distribution. Moreover, the first neglected term would lead to a divergent integral when $\Gamma_\ell(\omega)$ is integrated over all frequencies to obtain an approximation for $\gamma_\ell(t)$. The approximate convolution kernel derived from the three constants is, using (3.21),

$$\gamma_\ell(t) \simeq \frac{\Gamma_\ell(0)}{\pi} \int_0^\infty \exp(-\omega^2\sigma_\ell^2/2)\cos[\,\omega(t - \tau_\ell) + \omega^3\varrho_\ell^3/6\,]\,d\omega, \tag{3.31}$$

  $-\infty < t < +\infty$. This integral cannot be evaluated in closed form. However, for $\varrho_\ell = 0$ we obtain the symmetric Gaussian distribution,

$$\gamma_\ell(t) \simeq \frac{\Gamma_\ell(0)}{\sqrt{2\pi}\sigma_\ell} \exp\left[-\frac{(t - \tau_\ell)^2}{2\sigma_\ell^2}\right], \quad -\infty < t < +\infty. \tag{3.32}$$

  $\Gamma_\ell(\omega)$ has singularities (infinities) in both ω-halfplanes. Therefore $\gamma_\ell(t)$ is non-causal. This is avoided in the next example.

- **Gamma distribution**
  The transfer function

$$\Gamma_\ell(\omega) \simeq \frac{\Gamma_\ell(0)}{(1 + i\omega/\beta_\ell)^{\alpha_\ell}}, \quad \alpha_\ell \geq 1, \quad \beta_\ell > 0, \tag{3.33}$$

  which is analytic in the lower ω-halfplane, leads to a causal convolution function. $\Gamma_\ell(\omega)$ disposes only of the two parameters α_ℓ and β_ℓ and reproduces the first three terms of (3.28) by choosing

$$\alpha_\ell = (\tau_\ell/\sigma_\ell)^2, \quad \beta_\ell = \tau_\ell/\sigma_\ell^2.$$

  Since $\sigma_\ell \leq \tau_\ell$ [see (3.67)], we have in fact $\alpha_\ell \geq 1$. The skewness is already fixed, $\varrho_\ell^3 = 2\alpha_\ell/\beta_\ell^3 = 2\sigma_\ell^4/\tau_\ell$. The convolution function resulting from (3.33) is the Gamma distribution

$$\gamma_\ell(t) \simeq \frac{\Gamma_\ell(0)\,(\beta_\ell t)^{\alpha_\ell}}{\Gamma(\alpha_\ell)t} \exp(-\beta_\ell t), \quad t \geq 0. \tag{3.34}$$

An example comparing the different approximations is given in Fig. 3.– Other possible causal two-parameter distributions are the lognormal and the Weibull distribution.

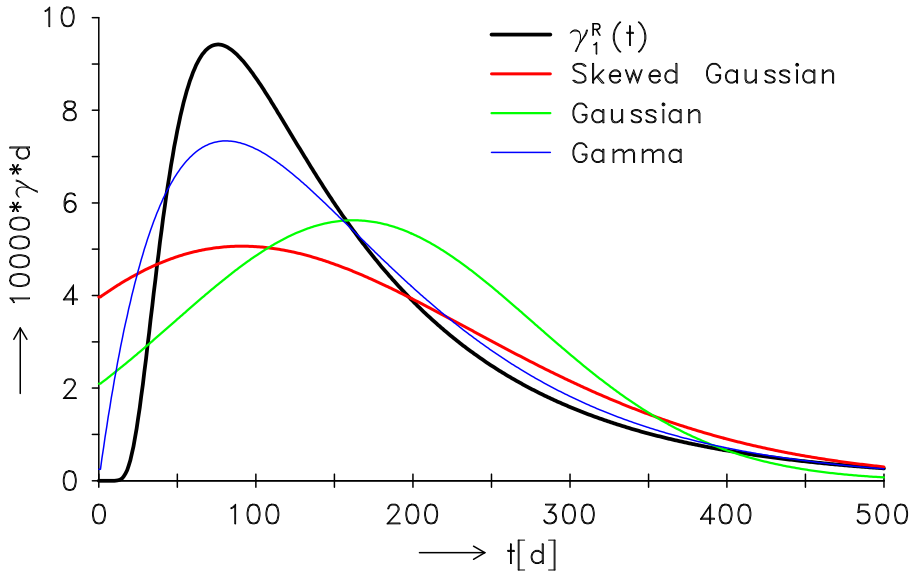

Figure 3: The convolution function $\gamma_1^R(t)$ from Fig. 2 and its approximations by the skewed Gaussian distribution (3.31), the Gaussian distribution (3.32) and the Gamma distribution (3.34). The non-causal Gaussian distributions have long tails for $t < 0$ and therefore the amplitudes in $t > 0$ are diminished.

3.2. Diffusion pattern of radial and tangential magnetic components

The geophysical significance of radial and tangential time constants will now be illustrated by transforming (2.18) into the time domain. We use again the conductivity distribution of Fig. 1 and assume as source at the CMB

$$S_\ell^{SV}(\vartheta,\varphi,\omega) = \frac{T}{2}\cdot\frac{\mathrm{e}^{-ix}\,\sin x}{x(1-x^2/\pi^2)}\cdot P_\ell(\cos\vartheta), \quad x := \omega T/2,$$

corresponding in the time domain to

$$S_\ell^{SV}(\vartheta,\varphi,t) = \begin{cases} \sin^2(\pi t/T)\cdot P_\ell(\cos\vartheta), & 0\le t\le T,\\ 0, \quad \text{else}, \end{cases} \tag{3.35}$$

which is a soft B_r-impulse of duration T with maximum value 1 at $t = T/2$.

Presented are results for $T = 200$ d and $\ell = 1$. Fig. 4 shows the time variatiom of the radial (red / thick) and tangential (blue / thin) component at the CMB (bottom) and at the surface of the Earth (top). In the center are displayed – in reverse time – the convolution kernels $\gamma_\ell^{R,T}(t)$, which link the fields at $r = c$ and $r = a$ via the convolution integral (3.20). The presentation is fully linear and therefore is not easily reconciled with the double-logarithmic plot in Fig. 2 containing the same information. [The convolution is performed by shifting the central panel to the left (say). For a fixed position of this panel, coinciding ordinates of the central and bottom panel are multiplied and integrated. The result is assigned in the top panel to that time, which is the (constant) sum of coinciding times in the central and bottom panel, e.g. $t = 500\ d$ in Fig. 4.] The components are shown at those colatitudes, which report at the surface the greatest positive values, i.e. for $B_{\ell r}$ at $\vartheta = 0$ and for $B_{\ell\vartheta}$ at $\vartheta = 90°$.

Whereas at the CMB the radial component shows the unipolar variation (3.35), the predominantly induced tangential component is bipolar: Broadly speaking, the ascending branch of $B_{\ell r}$ induces $B_{\ell\vartheta} > 0$ and $B_{\ell\vartheta} < 0$ is induced by the descending branch. Since $B_{\ell\vartheta}$ depends on the slope of $B_{\ell r}$, the maximum of $B_{\ell\vartheta}$ occurs earlier than the maximum of $B_{\ell r}$. The difference increases with increasing duration T. Very different convolution kernels $\gamma_\ell^R(t)$ and $\gamma_\ell^T(t)$ are required, such that after convolution both components – which at $r = a$ are derived from a scalar potential – agree in time and differ only by a space-dependent factor (top panel). In particular the long tail of $\gamma_\ell^T(t)$ achieves that the negative values of $B_{\ell\vartheta}(c)$ are always outweighed by the positive values.- For $T \to 0$ the maxima of $B_{\ell r}$ and $B_{\ell\vartheta}$ occur simultaneously: at the CMB at $t \simeq 0$ and at the surface at the maximum of $\gamma_\ell^R(t)$, i.e. at $t = 76$ d. With longer pulse duration increases the lead of the tangential component w.r.t the radial component from $\simeq 30$ d for $T = 200$ d to $\simeq 300$ d for $T = 2000$ d and $\simeq 700$ d for $T = 20000$ d.

The B_r-impulse at $r = c$ creates a magnetic field at $r = a$, where both components attain their maxima simultaneously. The time lag between these maxima and the maximum of the B_r impulse is the relevant delay time of the impulse. Fig. 4 shows that the maximum of the tangential component at the CMB occurs prior to the maximum of the radial impulse, which leads to a longer delay time for this component. These delay times $\tau^R_{\ell<}$ and $\tau^T_{\ell<}$ (with $\ell = 1$) are given in Table 1. They are lower bounds of the low-frequency delay times τ^R_ℓ and τ^T_ℓ introduced in Sect. 3.1. This low-frequency limit requires $\tau^{R,T}_\ell \ll T$.

T[d]	$\tau^R_{1<}$[d]	$\tau^T_{1<}$[d]
0	76	76
20	76	79
50	78	85
100	83	98
200	99	130
500	129	207
1000	148	307
2000	157	462
5000	161	699
10000	162	805
∞	162	857

Table 1: Convergence of $\tau^{R,T}_{1<}$ to $\tau^{R,T}_1$ with $\tau^{R,T}_1$ read from Table 2. For $T \to 0$ both maxima occur at the mode of $\gamma^R_1(t)$.

3.3. Determination of the time constants for given $\sigma(r)$

In this section it is shown how the three mantle time constsnts τ_ℓ, σ_ℓ and ϱ_ℓ can be determined from a given $\sigma(r)$. Via (3.27) and (3.24) the time constants are connected with the k-th derivative of $\Gamma_\ell(\omega)$ at $\omega = 0$. Since the definitions (2.14) and (2.15) of $\Gamma^R_\ell(\omega)$ and $\Gamma^T_\ell(\omega)$ involve field ratios only, we can select for f_ℓ a convenient normalization. For Γ^R_ℓ we choose $f_\ell(r,\omega) =: f^R_\ell(r,\omega)$ with $f^R_\ell(c,\omega) = 1$, whereas for Γ^T_ℓ we select $f_\ell(r,\omega) =: f^T_\ell(r,\omega)$ with $d f^T_\ell(r,\omega)/dr|_{r=c} = -\ell/c$. Taking into account that $f'_\ell(a) = -(\ell/a)\, f_\ell(a)$, Eqs. (2.14) and (2.15) are transformed into

$$\Gamma^R_\ell(\omega) = (c/a)^2\, f^R_\ell(a,\omega), \quad f^R_\ell(c,\omega) = 1, \tag{3.36}$$

$$\Gamma^T_\ell(\omega) = (c/a)^2\, f^T_\ell(a,\omega), \quad d f^T_\ell(r,\omega)/dr|_{r=c} = -\ell/c. \tag{3.37}$$

The potentials $f^{R,T}_\ell(r,\omega)$ satisfy as solutions of (2.10) the integral equation

$$f^{R,T}_\ell(r,\omega) = \left(\frac{c}{r}\right)^\ell - i\omega \int_c^a \sigma(x)\, G^{R,T}_\ell(r|x)\, f^{R,T}_\ell(x,\omega)\, dx, \tag{3.38}$$

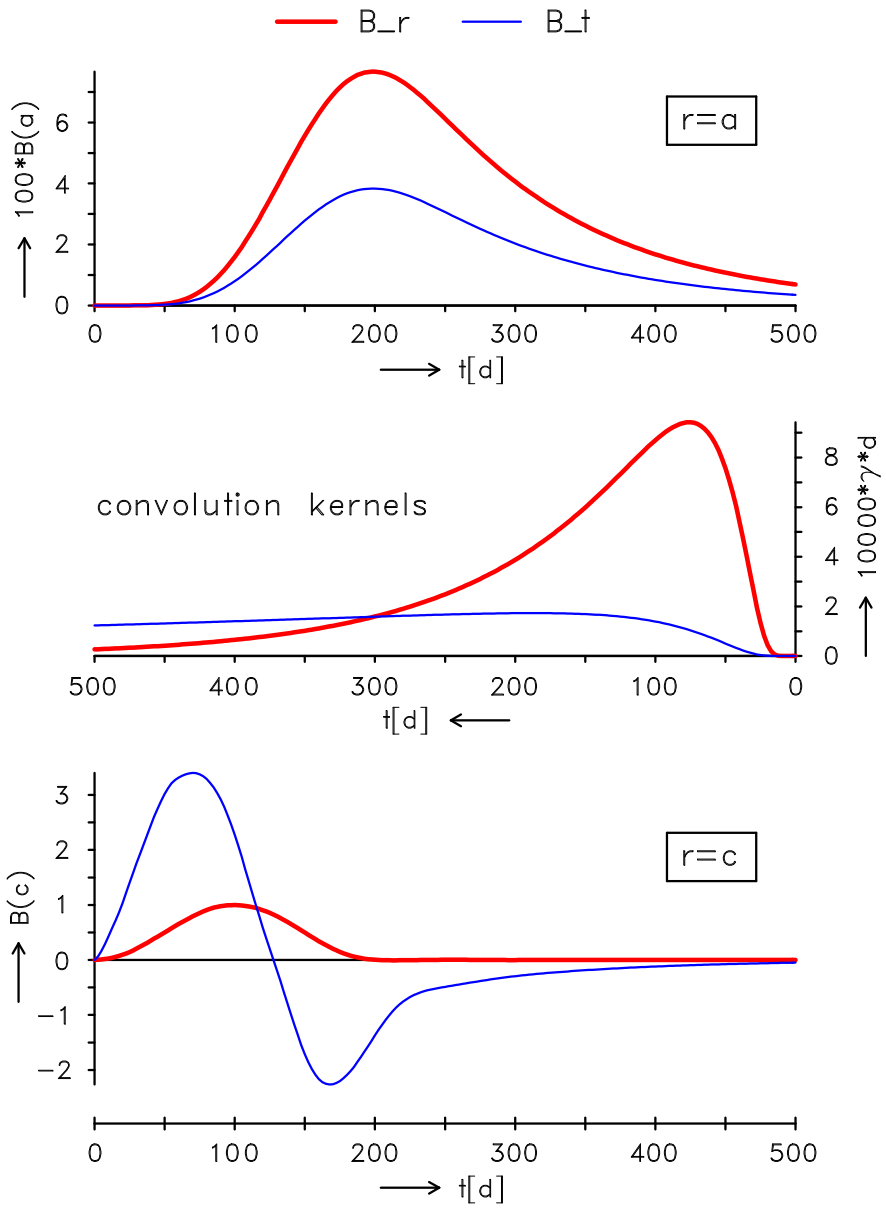

Figure 4: Degree $\ell = 1$, impulse duration $T = 200$ d: Diffusion of radial (red / thick) and tangential (blue / thin) magnetic components from the CMB ($r = c$) to the surface of the Earth ($r = a$). Used is the conductivity model of Fig. 1. See text for details.

where Green's function $G_\ell^{R,T}(r|r_0)$ solves the differential equation

$$\left[\frac{d^2}{dr^2} - \frac{\ell(\ell+1)}{r^2}\right] G_\ell^{R,T}(r|r_0) = -\mu_0\,\delta(r-r_0), \tag{3.39}$$

subject to the boundary conditions

$$G_\ell^R(c|r_0) = G_\ell^R(r|c) = 0, \quad dG_\ell^T(r|r_0)/dr|_{r=c} = dG_\ell^T(r|r_0)/dr_0|_{r_0=c} = 0. \tag{3.40}$$

These conditions grant the satisfaction of the boundary conditions for $f_\ell^{R,T}(r)$ at $r = c$, see Eqs. (3.36) and (3.37). Therefore

$$G_\ell^{R,T}(r|r_0) = \left(\frac{r_<}{r_>}\right)^\ell \cdot G_\ell^{R,T}(r_<|r_<) =: \left(\frac{r_<}{r_>}\right)^\ell \cdot g_\ell^{R,T}(r_<), \tag{3.41}$$

where $r_< := \min(r, r_0)$, $r_> := \max(r, r_0)$ and

$$g_\ell^R(r) = \frac{\mu_0\,c}{2\ell+1} \cdot \left[\frac{r}{c} - \left(\frac{c}{r}\right)^{2\ell}\right], \qquad g_\ell^T(r) = \frac{\mu_0\,c}{2\ell+1} \cdot \left[\frac{r}{c} + \frac{\ell+1}{\ell}\left(\frac{c}{r}\right)^{2\ell}\right]. \tag{3.42}$$

For brevity we omit from now on the superscripts R, T, but keep in mind that – due to the different forms of g_ℓ in (3.42) – different expressions hold for the diffusion of the radial and tangential magnetic component.

The potential $f_\ell(r,\omega)$ is an analytical function of ω in the circle $|\omega| < \lambda_{\ell 1}$, where $i\lambda_{\ell 1}$ is the pole of $\Gamma_\ell(\omega)$ with smallest modulus (see Sect. 3.4). Therefore, there exists in a small neighbourhood of $\omega = 0$ the power series

$$f_\ell(r,\omega) = \left(\frac{c}{a}\right)^\ell \sum_{k=0}^{\infty} \frac{(-i\omega)^k}{k!}\psi_{\ell k}(r), \tag{3.43}$$

with

$$\psi_{\ell k}(r) := \left(\frac{a}{c}\right)^\ell \cdot \left.\frac{d^k f_\ell(r,\omega)}{d(-i\omega)^k}\right|_{\omega=0}. \tag{3.44}$$

Recalling that $\Gamma_\ell(0) = (c/a)^{\ell+2}$, we deduce from (3.24), (3.36) and (3.37) that $m_{\ell k} = \psi_{\ell k}(a)$. Therefore (3.27) yields

$$\tau_\ell = \psi_{\ell 1}(a), \quad \sigma_\ell^2 = \psi_{\ell 2}(a) - \psi_{\ell 1}^2(a), \quad \varrho_\ell^3 = \psi_{\ell 3}(a) - 3\psi_{\ell 2}(a)\psi_{\ell 1}(a) + 2\psi_{\ell 1}^3(a). \tag{3.45}$$

By inserting (3.43) into the integral equation (3.38) and comparing the coefficients of equal powers of $-i\omega$, we obtain the the recursion

$$\psi_{\ell,k+1}(r) = (k+1)\int_c^a \sigma(x)\,G_\ell(r|x)\,\psi_{\ell k}(x)\,dx, \quad k = 0, 1, 2, \ldots. \tag{3.46}$$

The recursion starts with $\psi_{\ell 0}(r) = (a/r)^{\ell}$. The three subsequent terms are

$$\psi_{\ell 1}(r) = \int_c^a dx\, \sigma(x)\, G_\ell(r|x)\, (a/x)^{\ell}, \tag{3.47}$$

$$\psi_{\ell 2}(r) = 2 \int_c^a dx\, \sigma(x)\, G_\ell(r|x) \int_c^a dy\, \sigma(y)\, G_\ell(x|y)\, (a/y)^{\ell}, \tag{3.48}$$

$$\psi_{\ell 3}(r) = 6 \int_c^a dx\, \sigma(x)\, G_\ell(r|x) \int_c^a dy\, \sigma(y)\, G_\ell(x|y) \int_c^a dz\, \sigma(z)\, G_\ell(y|z)\, (a/z)^{\ell}. \tag{3.49}$$

The time constants τ_ℓ, σ_ℓ and ϱ_ℓ are according to (3.45) expressible in terms of $\psi_{\ell k}(a)$, $k = 1, 2, 3$. The evaluation, performed in Appendix A, yields

$$\tau_\ell = \int_c^a dx\, \sigma(x)\, G_\ell(x|x), \tag{3.50}$$

$$\sigma_\ell^2 = \int_c^a dx\, \sigma(x) \int_c^a dy\, \sigma(y)\, G_\ell^2(x|y), \tag{3.51}$$

$$\varrho_\ell^3 = 2 \int_c^a dx\, \sigma(x) \int_c^a dy\, \sigma(y) \int_c^a dz\, \sigma(z)\, G_\ell(x|y)\, G_\ell(y|z)\, G_\ell(z|x). \tag{3.52}$$

In terms of the partial Green's functions $g_\ell(r)$ defined in (3.42) a possible representation is

$$\tau_\ell = \int_c^a dx\, \sigma(x)\, g_\ell(x), \tag{3.53}$$

$$\sigma_\ell^2 = 2 \int_c^a dx\, \sigma(x)\, g_\ell^2(x) \int_x^a dy\, \sigma(y)\, (x/y)^{2\ell}, \tag{3.54}$$

$$\varrho_\ell^3 = 12 \int_c^a dx\, \sigma(x)\, g_\ell^2(x) \int_x^a dy\, \sigma(y)\, g_\ell(y) \int_y^a dz\, \sigma(z)\, (x/z)^{2\ell}. \tag{3.55}$$

Numerical values of the time constants derived from the model Fig. 1 are given in Table 2.

ℓ	τ_ℓ^R [d]	σ_ℓ^R [d]	ϱ_ℓ^R [d]	τ_ℓ^T [d]	σ_ℓ^T [d]	ϱ_ℓ^T [d]
1	162.1	114.7	141.6	857.1	771.5	969.7
2	129.9	85.3	104.1	395.8	320.1	399.6
3	107.5	65.6	79.0	250.4	183.3	226.3
4	91.3	52.0	61.7	181.1	121.3	147.8
5	79.2	42.2	49.4	141.2	87.4	104.9
6	69.8	35.1	40.4	115.4	66.6	78.8
7	62.3	29.7	33.7	97.5	52.9	61.7
8	56.4	25.5	28.5	84.3	43.2	49.8
9	51.4	22.2	24.5	74.2	36.2	41.2
10	47.2	19.5	21.3	66.2	30.8	34.7
11	43.7	17.3	18.7	59.8	26.7	29.7
12	40.6	15.6	16.5	54.4	23.4	25.8
13	38.0	14.1	14.8	50.0	20.7	22.6
14	35.6	12.8	13.3	46.2	18.5	20.1
15	33.6	11.7	12.0	42.9	16.7	17.9

Table 2: Radial and tangential ellectromagnetic time constants for the conductivity model of Fig. 1

.

Since $g_\ell^R < g_\ell^T$, we always have $\tau_\ell^R < \tau_\ell^T$, $\sigma_\ell^R < \sigma_\ell^T$ and $\varrho_\ell^R < \varrho_\ell^T$. The striking difference in the weight functions g_ℓ^R and g_ℓ^T is their behaviour close to the CMB. Here, a well-conducting layer will significantly affect the diffusion of tangential components (i.e. τ_ℓ^T), whereas it has negligible influence on the diffusion of B_r (i.e. τ_ℓ^R). The physical reason for this finding is that image currents induced in the close highly conducting core strongly damp the radial magnetic component, whereas the core enhances the induced tangential magnetic components **between** the layer and the CMB (but weakens them above the layer).

Discussion

Table 2 shows that for a reasonable conductivity distribution in the mantle, the time constants for the radial magnetic component do not exceed half a year. A significant impact of mantle conductivity on the diffusion of the SV only exists, if the SV has strong contributions with a time scale comparable with the time constants. If for a degree ℓ the SV does not change much over the width (corresponding to the smoothing time σ_ℓ) of the convolution kernel $\gamma(t)$ used in (3.20) and displayed in Fig. 2, one would observe at $r = a$ only a replica of the the SV at $r = c$, reduced by the factor $(c/a)^{\ell+2}$ and – at most – time-shifted by the small delay time τ_ℓ. Inversely, the observed SV continued to the CMB will have an amplitude increased by the factor $(a/c)^{\ell+2}$ and advanced by τ_ℓ.

3.4. Relationship between τ_ℓ, σ_ℓ, ϱ_ℓ and the free-decay times

The poles of $\Gamma_\ell^{R,T}(\omega)$ are those imaginary frequencies $\omega_{\ell j} = i\lambda_{\ell j}$, $\lambda_{\ell j} > 0$, $j = 1, 2, 3, \ldots$, for which (2.10) has eigensolutions with the boundary conditions

$$f_\ell^{R,T}(r,\omega) \to 0 \quad \text{for} \quad r \to \infty \quad \text{and} \quad f_\ell^R(c,\omega) = d\, f_\ell^T(r,\omega)/dr|_{r=c} = 0. \tag{3.56}$$

For the conductivity model of Fig. 1 the corresponding times $T_{\ell j} := 1/\lambda_{\ell j}$ are given in Table 3.

	$T_{\ell j}^R$ [d]				$T_{\ell j}^T$ [d]			
j	$\ell = 1$	$\ell = 2$	$\ell = 3$	$\ell = 4$	$\ell = 1$	$\ell = 2$	$\ell = 3$	$\ell = 4$
1	112.09	82.17	62.13	48.24	769.68	316.92	179.14	116.54
2	21.97	20.20	18.42	16.70	49.87	42.38	35.93	30.51
3	8.68	8.38	8.04	7.69	14.28	13.50	12.68	11.83
4	4.64	4.55	4.44	4.32	6.41	6.23	6.04	5.83
5	2.71	2.67	2.63	2.59	3.73	3.67	3.61	3.53
6	1.94	1.92	1.90	1.87	2.32	2.28	2.25	2.21
7	1.42	1.41	1.40	1.39	1.64	1.63	1.61	1.59
8	1.06	1.06	1.05	1.04	1.18	1.18	1.17	1.16
9	0.82	0.81	0.81	0.80	0.92	0.91	0.91	0.90
10	0.67	0.66	0.66	0.66	0.72	0.71	0.71	0.71

Table 3: The first poles $\omega_{\ell j} = i/T_{\ell j}$ of Γ_ℓ^R (at left) and Γ_ℓ^T (at right) for the conductivity model Fig. 1. The times $T_{\ell j}^R$ are also the decay times of freely decaying current sytems in the mantle.

The computation of free-decay modes of mantle currents requires the determination of the eigensolutions of (2.10) with the boundary conditions

$$f_\ell(r,\omega) \to 0 \quad \text{for} \quad r \to \infty \quad \text{and} \quad f_\ell(c,\omega) = 0. \tag{3.57}$$

These conditions agree with those applied to $f_\ell^R(r,\omega)$. Therefore the times $T_{\ell j}^R$ are also the free-decay times.

For radial quantum numbers $j \gg 1$ and a *smooth* conductivity variation $\sigma(r)$, the eigenvalues follow simple asymptotic rules. Let

$$T_0 := \left[\int_c^a \sqrt{\mu_0 \sigma(r)}\, dr \right]^2 .$$

Then for $j \gg 1$ (cf. Morse & Feshbach 1953, p. 739)

$$T^R_{\ell j} \simeq \frac{T_0}{(j-\frac{1}{2})^2\pi^2}, \quad T^T_{\ell j} \simeq \frac{T_0}{(j-1)^2\pi^2}.$$

In this first order approximation the quantum number ℓ plays no role.

Simple relationships exist between τ_ℓ, σ_ℓ, ϱ_ℓ and the pole positions $i\lambda_{\ell j} = i/T_{\ell j}$,

$$\boxed{\tau_\ell = \sum_{j=1}^{\infty} T_{\ell j}, \quad \sigma_\ell^2 = \sum_{j=1}^{\infty} T_{\ell j}^2, \quad \varrho_\ell^3 = 2\sum_{j=1}^{\infty} T_{\ell j}^3} \tag{3.58}$$

We shall sketch the proof of (3.58): Let

$$\varphi_{\ell j}(r) := f_\ell(r, i\lambda_{\ell j})$$

be the eigenfunctions defined by (3.56). They satisfy the orthonormalization

$$\int_c^a \sigma(r)\,\varphi_{\ell j}(r)\,\varphi_{\ell k}(r)\,dr = \delta_{jk}, \tag{3.59}$$

where δ_{jk} is the Kronecker symbol, and the integral equation [= homogeneous version of (3.38)]

$$\varphi_{\ell j}(r) = \lambda_{\ell j} \int_c^a \sigma(x)\,G_\ell(r|x)\,\varphi_{\ell j}(x)\,dx \tag{3.60}$$

with Green's function $G_\ell(r|x)$ given in (3.41) and (3.42). Now $G_\ell(r|x)$ is expanded w.r.t. to the variable x in terms of the eigenfunctions $\varphi_{\ell j}(x)$,

$$G_\ell(r|x) = \sum_{j=1}^{\infty} c_j(r)\,\varphi_{\ell j}(x). \tag{3.61}$$

Using (3.59) and (3.60), we obtain as expansion coefficients

$$c_j(r) = \int_c^a \sigma(x)\,G_\ell(r|x)\,\varphi_{\ell j}(x)\,dx = \frac{\varphi_{\ell j}(r)}{\lambda_{\ell j}} \tag{3.62}$$

and therefore the bilinear expansion of the kernel is

$$G_\ell(r|x) = \sum_{j=1}^{\infty} \frac{\varphi_{\ell j}(r)\,\varphi_{\ell j}(x)}{\lambda_{\ell j}}. \tag{3.63}$$

Mercer's theorem (Courant & Hilbert 1968, p. 117) guarantees that this expansion exists and converges absolutely and uniformly. Let the iterated Green's functions $G_\ell^{(n)}(r|x)$ be defined by

$$G_\ell^{(1)}(r|x) := G_\ell(r|x), \quad G_\ell^{(n+1)}(r|x) := \int_c^a du\, \sigma(u)\, G_\ell(r|u)\, G_\ell^{(n)}(u|x), \quad n \geq 1. \tag{3.64}$$

Then insertion of (3.63) into (3.64) yields on using the orthogonality (3.59), cf. Courant & Hilbert 1968, p. 117,

$$G_\ell^{(n)}(r|x) = \sum_{j=1}^{\infty} \frac{\varphi_{\ell j}(r)\, \varphi_{\ell j}(x)}{\lambda_{\ell j}^n}. \tag{3.65}$$

The integral representations (3.50) to (3.52) admit the formulation

$$\tau_\ell = \int_c^a \sigma(x)\, G_\ell^{(1)}(x|x)\, dx, \quad \sigma_\ell^2 = \int_c^a \sigma(x)\, G_\ell^{(2)}(x|x)\, dx, \quad \varrho_\ell^3 = 2 \int_c^a \sigma(x)\, G_\ell^{(3)}(x|x)\, dx. \tag{3.66}$$

Therefore the insertion of (3.65) into (3.66) leads on using (3.59) to (3.58).

From (3.58) follows

$$\tau_\ell^2 - \sigma_\ell^2 = \sum_{\substack{j,k=1 \\ j \neq k}}^{\infty} T_{\ell j} T_{\ell k} \geq 0.$$

Hence,

$$\boxed{T_{\ell 1} \leq \sigma_\ell \leq \tau_\ell} \tag{3.67}$$

Equality only holds for a single thin shell of conductance Σ at $r = b$, $c \leq b \leq a$, where only one pole exists and therefore all three times compared in (3.67) agree. From (3.50) to (3.52) follows with $\sigma(r) = \delta(r - b) \cdot \Sigma$ and $G_\ell(b|b) = g_\ell(b)$

$$T_{\ell 1} = \tau_\ell = \sigma_\ell = g_\ell(b) \cdot \Sigma$$

and $\varrho_\ell = \sqrt[3]{2}\, g_\ell(b) \cdot \Sigma$. The corresponding convolution function is simply

$$\gamma_\ell(t) = \Gamma_\ell(0) \exp(-t/\tau_\ell)/\tau_\ell,$$

i.e. the Gamma distribution (3.34) with $\alpha_\ell = 1$ and $\beta_\ell = 1/\tau_\ell$.

References

Backus, G.E., 1983. Application of mantle filter theory to the magnetic jerk of 1969, *Geophys. J. R. astr. Soc.*, **74**, 713-746.

Ballani, L., Greiner-Mai, H. & Stromeyer, D., 2002. Determining the magnetic field in the core-mantle boundary zone by non-harmonic downward continuation, *Geophys. J. Int.*, **149**, 374-389.

Benton, E.R. & Whaler, K.A., 1983. Rapid diffusion of the poloidal geomagnetic field through the weakly conducting mantle: a perturbation solution, *Geophys. J. R. astr. Soc.*, **75**, 77-100.

Courant, R. & Hilbert, D., 1968. *Methoden der Mathematischen Physik I*, 3rd ed., Springer-Verlag, Heidelberg [etc.].

Fisz, M., 1976. *Wahrscheinlichkeitsrechnung und mathematische Statistik*, 8th ed., VEB Deutscher Verlag der Wissenschaften, Berlin.

Holme, R., 1998. Electromagnetic core-mantle coupling – I. Explaining decadal changes in the length of day, *Geophys. J. Int.*, **132**, 167-180.

McDonald, K.L., 1957. Penetration of the geomagnetic secular variation through a mantle with variable conductivity, *J. Geophys. Res.*, **63**, 117-141.

Morse, P.M. & Feshbach, H., 1953. *Methods of theoretical physics*, Vol. 1, McGraw-Hill, New York.

A. Evaluation of the integrals defining the time constants

The time constants τ_ℓ, σ_ℓ and ϱ_ℓ are given by (3.45) and (3.46). In the sequel repeated use is made of the definition (3.41) of Green's function and its symmetry $G_\ell(x|y) = G_\ell(y|x)$.

a) Delay time τ_ℓ:

$$\tau_\ell = \psi_{\ell 1}(a) = \int_c^a dx\,\sigma(x)\,G_\ell(a|x)\,(a/x)^\ell = \int_c^a dx\,\sigma(x)\,G_\ell(x|x) = \int_c^a dx\,\sigma(x)\,g_\ell(x),$$

which agrees with (3.50) and (3.53).

b) Smoothing time σ_ℓ:
Let

$$\int dV_2\, f(x,y) := \int_c^a dx\,\sigma(x) \int_c^a dy\,\sigma(y)\, f(x,y).$$

Moreover let $\Theta(x)$ with $\Theta(x)+\Theta(-x) = 1$ be Heaviside's step function. Then (3.45) yields

$$\sigma_\ell^2 = \psi_{\ell 2}(a) - \tau_\ell^2 = I_1 + I_2$$

with

$$\begin{aligned}
I_1 &:= 2\int dV_2\, G_\ell(a|x)\, G_\ell(x|y)\, (a/y)^\ell\, \Theta(x-y) - \tau_\ell^2 \\
&= \int dV_2\, G_\ell(x|x)\, G_\ell(y|y)\, [\, 2\Theta(x-y) - 1\,] \\
&= \int dV_2\, G_\ell(x|x)\, G_\ell(y|y)\, [\Theta(x-y) + \Theta(y-x) - 1\,] = 0, \\
I_2 &:= 2\int dV_2\, G_\ell(a|x)\, G_\ell(x|y)\, (a/y)^\ell\, \Theta(y-x) = 2\int dV_2\, G_\ell^2(x|y)\, \Theta(y-x) \\
&= \int dV_2\, G_\ell^2(x|y)\, [\, \Theta(y-x) + \Theta(x-y)\,] = \int dV_2\, G_\ell^2(x|y).
\end{aligned}$$

Therefore

$$\sigma_\ell^2 = I_2 = \int dV_2\, G_\ell^2(x|y),$$

which agrees with (3.51), whereas (3.54) follows from the second part of the fourth line. In the third and fifth line the previous factors 2 are replaced by unity because an identical term is added by interchanging the dummy integration variables x and y and exploiting the symmetry in x and y of the remaining integrand.

c) Skewing time ϱ_ℓ:
Let

$$\int dV_3\, f(x,y,z) := \int_c^a dx\, \sigma(x) \int_c^a dy\, \sigma(y) \int_c^a dz\, \sigma(z)\, f(x,y,z).$$

Then (3.45) and (3.47) to (3.49) yield

$$\varrho_\ell^3 = \psi_{\ell 3}(a) - 3\tau_\ell[\, \psi_{\ell 2}(a) - \tau_\ell^2\,] - \tau_\ell^3 = \psi_{\ell 3}(a) - 3\tau_\ell\sigma_\ell^2 - \tau_\ell^3 = I_{11} + I_{12} + I_{21} + I_{22}$$

with

$$\begin{aligned}
I_{11} &:= 6\int dV_3\, G_\ell(a|x)\, G_\ell(x|y)\, G_\ell(y|z)\, (a/z)^\ell\, \Theta(x-y)\Theta(y-z) - \tau_\ell^3, \\
I_{12} &:= 6\int dV_3\, G_\ell(a|x)\, G_\ell(x|y)\, G_\ell(y|z)\, (a/z)^\ell\, \Theta(x-y)\Theta(z-y) - 3\tau_\ell\sigma_\ell^2, \\
I_{21} &:= 6\int dV_3\, G_\ell(a|x)\, G_\ell(x|y)\, G_\ell(y|z)\, (a/z)^\ell\, \Theta(y-x)\Theta(y-z), \\
I_{22} &:= 6\int dV_3\, G_\ell(a|x)\, G_\ell(x|y)\, G_\ell(y|z)\, (a/z)^\ell\, \Theta(y-x)\Theta(z-y).
\end{aligned}$$

These integrals admit considerable simplifications:

$$\begin{aligned}
I_{11} &= \int dV_3\, G_\ell(x|x)\, G_\ell(y|y)\, G_\ell(z|z)\, [\, 6\,\Theta(x-y)\Theta(y-z) - 1\,] \\
&= \int dV_3\, G_\ell(x|x)\, G_\ell(y|y)\, G_\ell(z|z)\, [\, 1 - 1\,] = 0, \\
I_{12} &= 6 \int dV_3\, G_\ell(x|x)\, G_\ell^2(y|z)\, [\, \Theta(x-y)\Theta(z-y) - \Theta(z-y)\,] \\
&= -6 \int dV_3\, G_\ell(x|x)\, G_\ell^2(y|z)\, \Theta(y-x)\Theta(z-y), \\
I_{21} &= 6 \int dV_3\, G_\ell^2(x|y)\, G_\ell(z|z)\, \Theta(y-x)\Theta(y-z) \\
&= 6 \int dV_3\, G_\ell(x|x)\, G_\ell^2(y|z)\, \Theta(z-y)\Theta(z-x), \\
I_{22} &= 6 \int dV_3\, G_\ell(x|y)\, G_\ell(y|z)\, G_\ell(z|x)\, \Theta(y-x)\Theta(z-y) \\
&= \int dV_3\, G_\ell(x|y)\, G_\ell(y|z)\, G_\ell(z|x).
\end{aligned}$$

In I_{11} and I_{22} Green's functions (and dV_3) are invariant under a permutation of (x, y, z). This allows us to replace a given ordering of x, y, z, spanning only a pyramid of volume $(a-c)^3/6$, by all six permutations spanning the whole cube $(a-c)^3$. – In I_{12} we have inserted σ_ℓ^2 in its form (3.54) [with (x, y) replaced by (y, z)]. Similarly in I_{21} the tripel (x, y, z) was replaced by (y, z, x) to allow a combination with I_{12},

$$\begin{aligned}
I_{21} + I_{12} &= 6 \int dV_3\, G_\ell(x|x)\, G_\ell^2(y|z)\, \Theta(z-y)\, [\, \Theta(z-x) - \Theta(y-x)\,] \\
&= 6 \int dV_3\, G_\ell(x|x)\, G_\ell^2(y|z)\, \Theta(z-x)\Theta(x-y) \\
&= 6 \int dV_3\, G_\ell(x|y)\, G_\ell(y|z)\, G_\ell(z|x)\, \Theta(z-x)\Theta(x-y) \\
&= \int dV_3\, G_\ell(x|y)\, G_\ell(y|z)\, G_\ell(z|x) = I_{22}.
\end{aligned}$$

Therefore

$$\varrho_\ell^3 = I_{11} + I_{12} + I_{21} + I_{22} = 2I_{22} = 2 \int dV_3\, G_\ell(x|y)\, G_\ell(y|z)\, G_\ell(z|x),$$

which agrees with (3.52). Finally (3.55) follows from the first form of I_{22} given above.